Developmental Cognitive Neuroscience 76 (2025) 101621

Contents lists available at ScienceDirect

Developmental Cognitive Neuroscience

journal homepage: www.elsevier.com/locate/dcn

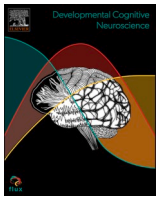

Functional organization of the allostatic interoceptive network in adolescence: Links to peer victimization and prospective depressive symptoms

Natalie G. Frye [a,*], Tehila Nugiel [b], Gabriella M. Alvarez [c], Mitch J. Prinstein [a], Jessica R. Cohen [a], Eva H. Telzer [a], Kristen A. Lindquist [a]

[a] Department of Psychology & Neuroscience, University of North Carolina at Chapel Hill, 235 East Cameron Ave, Chapel Hill, NC 27599, USA
[b] Department of Psychology, Florida State University, 1107 West Call Street, Tallahassee, FL 32304, USA
[c] Department of Psychology, University of Pittsburgh, 210 South Bouquet Street, Pittsburgh, PA 15260, USA

ARTICLE INFO

Keywords:
Depression
Adolescence
Functional connectivity
Allostasis
Rumination
Peer victimization

ABSTRACT

The present study examines the role of brain network organization in the prospective prediction of adolescent depressive symptoms and links to the social and psychological context. Using a path model with data from a larger longitudinal study of adolescents beginning in 6th-8th grade (N = 117, 55 % female, $M_{age\ at\ scan}$= 12.99), we first established that organizational properties of brain networks theoretically linked to depression predicted greater depressive symptoms two years later. Specifically, when controlling for gender and initial depression, greater global efficiency of the allostatic interoceptive network (AIN) and greater segregation of the frontoparietal network (FPN) from the salience network (SN) predicted depressive symptoms an average of two years later. Linking these neural findings to psychological individual differences, we found that self-reported rumination mediated the effect of AIN global efficiency on prospective depressive symptoms. We further linked these neural findings to the social context by demonstrating that greater self-reported relational peer victimization prospectively predicted AIN global efficiency. Collectively, these findings situate the emergence of adolescent depressive symptoms as a confluence of brain organization properties, perceived social rejection, and individual differences in rumination.

1. Introduction

It has long been observed that rates of clinical depression (Angold et al., 1998; Beesdo et al., 2009; Fergusson et al., 2007; Fleming et al., 1989; Kessler et al., 2005; Lewinsohn et al., 1993; McGee et al., 1992; Steinhausen and Winkler Metzke, 2003; Thapar et al., 2012) and depressive symptoms such as negative mood and anhedonia (Joinson et al., 2012) spike in prevalence during adolescence. Depression among adolescents in the U.S. is becoming more common, especially for girls (Daly, 2022). It is thus more and more imperative to understand the development of depression in adolescents, including both its neurobiological and social contributors.

1.1. The neurobiology of depression

The past three decades of research exploring the neural correlates of depression has often focused on identifying discrete brain areas, tracts, or local circuits that are associated with depressive symptomology or diagnosis. However, there have also been calls for network-based understandings of the neurobiology of depression, given growing evidence that the brain performs different functions via flexible, overlapping, context-dependent brain networks (Anderson, 2010; Noble et al., 2024; Westlin et al., 2023).

A prominent network-based approach to psychopathology (Menon, 2011) links aberrations of the salience network (SN), the default mode network (DMN), and the frontoparietal network (FPN) to the emergence of psychopathology via their involvement in psychological processes such as visceromotor responses to salient stimuli, self-referential and autobiographical processing, and cognitive control, respectively. For instance, in adults, depression has been associated with greater connectivity between regions in the FPN and the DMN and lower connectivity between regions in the FPN and the SN (Wu et al., 2020; Tang

* Corresponding author.
E-mail address: nfrye@unc.edu (N.G. Frye).

https://doi.org/10.1016/j.dcn.2025.101621
Received 5 June 2025; Received in revised form 30 August 2025; Accepted 24 September 2025
Available online 25 September 2025

et al., 2013; Veer et al., 2010; see Kaiser et al., 2015 for a meta-analysis). A recent mega-analysis of datasets containing adolescents and emerging adults found reduced connectivity within the DMN, between regions of the DMN and SN, and between regions of the FPN and SN when comparing participants with and without major depressive disorder (Tse et al., 2024).

Connectivity between the DMN and SN, which converge to create a large-scale network called the allostatic-interoceptive network (AIN), is particularly central to a recently proposed model of the neurobiology of depression (Shaffer et al., 2022). In addition to containing cortical aspects of the DMN and SN, the AIN contains areas such as the mid-cingulate cortex, parahippocampal gyrus, postcentral gyrus, and subcortical structures such as the periaqueductal gray, parabrachial nucleus, nucleus of the solitary tract, ventral striatum, and hypothalamus. Via these wide-ranging areas, the AIN is thought to use semantic and context-specific autobiographical memory representations (Andrews-Hanna et al., 2010; Barrett and Satpute, 2013; Raichle, 2015; Satpute and Lindquist, 2019) to initiate adaptive visceromotor changes in preparation for predicted threats and challenges in the environment. The AIN also represents afferent information from the viscera (Barrett et al., 2016; Barrett and Satpute, 2013) for the purpose of predictively regulating physiological and metabolic needs. Such predictive regulation of the body's internal state is called allostasis (Barrett and Simmons, 2015; Barrett et al., 2016; Shaffer et al., 2022) and the result is efficient energy use and adaptive sensory and motor processing in the face of changing external circumstances (Clark, 2013; Friston, 2010; Katsumi et al., 2022; Schulkin and Sterling, 2019; Sterling, 2012; Barrett and Simmons, 2015; Barrett et al., 2016). The allostatic interoceptive network allows the body to prepare for an external event that is predicted to be threatening (e.g., a looming person) or rewarding (e.g., a friendly face), by temporarily diverting glucose from regulatory activities (e.g., digestion) to energize the autonomic nervous system and skeleton-muscular system and prepare the body for action (e.g., running away v. approaching). In this predictive process, the brain must weigh internally-generated predictions against incoming prediction errors. When not optimally functioning, the allostatic interoceptive network may improperly weigh predictions (e.g., that someone is threatening) and ignore prediction errors (e.g., that they are in fact being kind). Allostatic dysregulation is thought to occur when the brain encounters stimuli that it has difficulty predicting over a long period of time, which causes an imbalance in the weighing of predictions, prediction error, and ultimately inefficient metabolic regulation (Shaffer et al., 2022). Over time, dysregulated allostasis can result in common symptoms of depression such as negative affect, fatigue, and withdrawal (Barrett et al., 2016; Shaffer et al., 2022).

1.2. Social adversity as a pathway to allostatic dysregulation and depression

In adolescence, the changing social landscape may be a source of allostatic dysregulation. It is well known that adverse experiences within peer relationships become particularly detrimental to adolescents' mental health due to the increasing salience and shifting complexity of those relationships in adolescence (Arseneault et al., 2010; Cowen et al., 1973). For instance, there are well-established links between experiencing rejection and exclusion from one's peer group and internalizing symptoms such as depression and loneliness (Heilbron and Prinstein, 2010; Hymel et al., 1990; Lochman and Wayland, 1994; see Choukas-Bradley and Prinstein, 2014 for a review). Experiences of more targeted adverse experiences with peers, such as exclusion by a specific peer or small group of peers (i.e., relational peer victimization) or receiving physical threats or aggression from specific peers (i.e., overt peer victimization) also predict internalizing symptoms (Crick and Grotpeter, 1996; Prinstein et al., 2001; Reijntjes et al., 2010, 2011; Vernberg, 1990) and depression (Wang et al., 2010).

Moreover, growing research demonstrates that adverse social experiences may become biologically embedded via their effects on allostasis. In humans, allostasis is not only an individual process but also a social process; social groups can conserve the metabolic resources of individuals when individuals co-regulate one another's' allostasis (Atzil et al., 2018; Beckes and Coan, 2011; Schulkin, 2011). Problems in social relationships therefore can disrupt an individual's allostasis, which has metabolic consequences (Saxbe et al., 2020; Theriault et al., 2021). Thus, it is possible that adverse peer experiences exert influences on depression in part because they impact allostasis and the function of the AIN. For instance, although no research has specifically examined the role of peer victimization on the AIN, peer victimization has been associated with enhanced neural activation in key nodes within the AIN such as the amygdala, dorsal anterior cingulate cortex, and anterior insula (McIver et al., 2018; Rudolph et al., 2016). Thus, after examining connections between the AIN and depression, the present study performed exploratory analyses to examine whether preceding experiences of social adversity can explain the brain organization metrics associated with later depressive symptoms.

1.3. The present study

The present paper uses a unique longitudinal data set of 117 adolescents from the rural southeastern U.S. who completed questionnaires, school-based sociometric assessments, and resting state neuroimaging when they were in 6th-8th grades to examine for the first time whether differences in organization of not only the DMN, SN, and FPN, but also the AIN, are prospectively associated with depressive symptoms. In preregistered analyses, we sought to replicate past findings implicating the SN and FPN in depression and establish a longitudinal link between AIN organization and depression. We furthermore examined whether AIN organization is prospectively linked to depression via increased brooding, a symptom of depression that might reflect over-weighting internally-generated predictions and bodily sensations. Finally, since all participants who completed neuroimaging in our sample had completed school-based sociometric assessments and questionnaires about their perceived degree of peer victimization on average seven months prior to neuroimaging, we performed an exploratory path analysis to examine whether aspects of adolescents' social context set the stage for patterns of brain organization associated with the development of later depressive symptoms.

To test these hypotheses, we used several graph theory-based network metrics to index the functional organization within and between a priori brain networks. These included global efficiency, which indexes the degree to which all nodes in a network are interconnected, or integration within a network; participation coefficient, which indexes the degree of integration between one network the rest of the brain; and system segregation, which indexes the degree to which there are more connections among nodes within a network and fewer connections between networks, or the degree to which networks are segregated from each other.

Past research has linked higher whole-brain global efficiency to depression in adolescents (Wu et al., 2020). Building off this finding as well as theory linking the AIN to depression (Shaffer et al., 2022), we hypothesized that greater global efficiency of the AIN would prospectively predict depression. We also included global efficiency of the FPN, given the FPN's involvement in cognitive control, and evidence that cognitive control is protective against depression (Davis et al., 2024; Rudolph et al., 2017). We hypothesized that higher participation coefficient of the AIN and the FPN with the rest of the brain would predict depressive symptoms. Building on prior work in adults showing that depression is associated with greater connectivity between regions in the FPN and the DMN and lower connectivity between regions in the FPN and the SN (Wu et al., 2020; Tang et al., 2013; Veer et al., 2010; see Kaiser et al., 2015 for a meta-analysis), we examined system segregation between each the FPN, DMN, and SN.

2. Methods and materials

2.1. Participants

As part of a parent longitudinal study, participants were recruited from three middle schools in the rural southeastern United States. Eight hundred seventy-three students from these middle schools completed in-school assessments in November and December of 2016, when they were in 6th-7th grade (timepoint 1; see Fig. 1). At this timepoint, participants responded to self-report measures and made sociometric nominations of their peers. A subset of these participants were then recruited to complete an additional portion of the study involving an fMRI scan. Participants were excluded for neurological conditions such as learning disorders, seizures, or head trauma but were not screened for mental health symptoms; see Appendix A for all exclusion criteria. One hundred forty-one participants completed a second session including a resting state fMRI scan and self-report assessments, which occurred between December 2016 and September 2017 (timepoint 2a; see Fig. 1). An additional cohort of 30 participants who were in 7th and 8th grade were also recruited to complete fMRI scans in November 2017 and September 2018 (timepoint 2b; see Fig. 1). This resulted in a total of 171 participants who completed the in-school behavioral assessment, including peer nominations, in timepoint 1 (T1) and who then participated in fMRI scanning and additional self-report assessments during timepoint 2 (T2). Finally, 145 participants returned for a third session that included an fMRI scan and self-report assessments, which occurred between November 2018 and November 2019 (timepoint 3; TP3; see Fig. 1). The present report used data from the in-school assessments in T1, fMRI and self-report data from T2, and self-report data from T3. T1 and T2 were on average seven months apart, and T2 and T3 were on average two years apart. Of the 171 participants who participated in fMRI scans in T2, 54 were excluded from our analyses due to not having a usable resting-state fMRI scan (see Appendix A for details).

The final sample of 117 adolescents included in our analyses had a mean age of 12.39 years at T1 (SD= 0.58), 12.99 years at T2 (SD= 0.56), and 14.74 years at T3 (SD= 0.59), was 55 % female, and came from diverse racial/ethnic (36.75 % Hispanic/Latine; 33.33 % White; 19.66 % Black; 8.55 % multi-racial; 1.71 % other) and socioeconomic backgrounds (Area Deprivation Index: *M*= 68.16, SD= 16.93, *range*= 33–97; see Appendix A for details). Participants and their parent/guardian(s) provided written assent/consent, according to the university's Institutional Review Board.

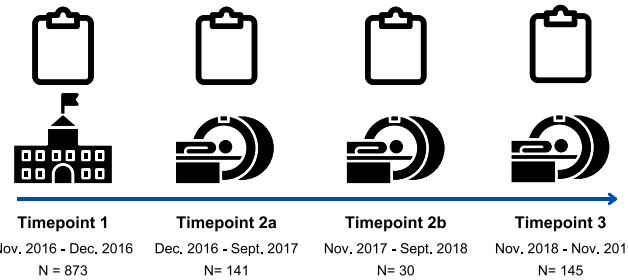

Fig. 1. Graphical depiction of data collection timepoints. Note: Timepoint 1 included self-report assessments and peer nominations that were later used to compute sociometric measures. Timepoint 2a included an fMRI scan and additional self-report assessment for a subset of 141 participants. Timepoint 2b included an fMRI scan and self-report assessments for an additional cohort of 30 participants who had participated in timepoint 1. Timepoint 3 included an fMRI scan and self-report assessments for 145 returning participants; however, we only used self-report data from this timepoint.

2.2. Measures

2.2.1. Demographics

Participants self-reported their sex, age at each timepoint, and race/ethnicity. Socioeconomic status was measured with the Area Deprivation Index (ADI; Kind and Buckingham, 2018), which is a measure of objective socioeconomic status that ranks U.S. neighborhoods (census block groups) by socioeconomic disadvantage using census data (see Appendix A for details). Pubertal development status was assessed only at T1 using the self-report Pubertal Development Scale (Petersen et al., 1988) (see Appendix A).

2.2.2. Short mood and feelings questionnaire: depressive symptoms

Depressive symptoms were assessed at each timepoint via a self-report questionnaire including nine items adapted from the Short Mood and Feelings Questionnaire (SMFQ; Angold et al., 1998). Participants responded about how they had felt in the past two weeks using a three-point scale (0 = *Not true*, 1 = *Sometimes true*, 2 = *Mostly true*). Items included: "I felt miserable or unhappy" and "I didn't enjoy anything at all." Depressive symptoms were calculated as the sum of the responses to all nine items, yielding good to excellent internal consistency at the three timepoints (Cronbach's α= 0.86, 0.89, 0.93).

2.2.3. Peer victimization

Self-reported peer victimization was assessed at T1 via a subset of questions from the Revised Peer Experiences Questionnaire (R-PEQ; Prinstein et al., 2001). This self-report questionnaire consists of 14 items and asks participants to rate how often they have had different experiences with their peers in the past two months using a five-point scale (1 = *Never*, 2 = *Once or twice*, 3 = *A few times*, 4 = *About once a week*, 5 = *A few times a week*). It contains subscales of overt peer victimization, which includes items such as "A teen threatened to hurt or beat me up" and "A teen hit, kicked, or pushed me in a mean way," and relational peer victimization, which includes items such as "A teen left me out of what they were doing" and "A teen did not invite me to a party or social event even though they knew that I wanted to go." Overt victimization scores were calculated as a sum of the three items included in the overt subscale, and relational victimization scores were calculated as a sum of the three items in the relational subscale. The overt victimization scale yielded acceptable internal consistency (Cronbach's α= 0.70), and the relational victimization scale yielded questionable internal consistency (Cronbach's α= 0.67).

2.2.4. Sociometric ratings of peer acceptance and rejection

During the in-school assessment at T1, participants were given the full roster of students in their school and grade level and asked to nominate an unlimited number of their peers who they liked most and liked least. See Appendix A for additional details. *Social preference* scores were calculated for each individual using the like/dislike nominations. To do this, both "like most" and "like least" nominations were z-scored so that they indicated a relative position compared to other students in their grade. Next, difference scores were computed for each participant to produce a measure of social preference (z-score of "liked least" subtracted from z-score of "liked most"), where a higher score indicated being more well-liked or accepted by peers. Sociometric social preference scores are a robust index of social acceptance (i.e. high social preference score) and rejection (i.e. low social preference score) from peers (Prinstein, 2017).

2.2.5. Ruminative response styles questionnaire: brooding subscale

A measure of rumination was used in exploratory analyses, and it was assessed at T3 by the Brooding subscale of the Ruminative Response Styles Questionnaire (Treynor et al., 2003). Participants responded on a four-point scale (1 = *Almost never*, 2 = *Sometimes*, 3 = *Often*, 4 = *Almost always*) to indicate how often they generally do things such as "Think 'What am I doing to deserve this?'," and "Think about a recent situation,

wishing it had gone better." Rumination was calculated as the sum of the five items in the brooding subscale, yielding good internal consistency (Cronbach's α= 0.88).

2.3. MRI data acquisition and analysis

Imaging data were acquired using a 3-Tesla Siemens Prisma MRI scanner. During scanning, participants completed an eight-minute long resting-state scan. During the resting state scan, 240 T2*-weighted echoplanar images (EPI) were obtained (repetition time [TR]= 2 s; echo time [TE]= 25 ms; field of view [FOV]= 230 mm; 92 ×92 matrix; voxel size= 2.5 ×2.5x3mm^3; flip angle= 90 degrees; 37 slices; slice thickness= 3 mm). A structural scan was also obtained for purposes of registration. A T1-weighted magnetization-prepared rapid-acquisition gradient echo anatomical scan was obtained (MPRAGE; TR= 1.9 s; TE= 2.3 ms; FOV= 230 mm; 256 ×256 matrix; sagittal plane; 192 slices; slice thickness=1 mm). The orientation for EPI scans was oblique axial to maximize brain coverage and to reduce noise. Data from these resting-state scans have previously been reported in Do et al. (2022).

MRI data preprocessing was conducted using *fMRIprep* v1.5.3 (Esteban et al., 2019; RRID:SCR_016216; see Appendix A for details) and postprocessed using the pipeline *clpipe* (v1.4.3; Henry et al., 2022), which included regression of head motion using 32 parameters (3 translation parameters, 3 rotation parameters, CSF and WM timeseries, and their quadratic terms, first temporal derivatives, and temporal derivatives of quadratic terms), high pass filtering at.008 Hz, respiratory notch filtering of the framewise displacement (FD) timeseries at 0.31–0.43 Hz, intensity normalization, and scrubbing of motion-outlier timepoints with notch-filtered FD greater than 0.3 while requiring five contiguous non-scrubbed timepoints. Scans with a mean FD of > .50 mm before scrubbing were also excluded.

2.3.1. Functional connectivity analyses

Region of interest (ROI) extraction was performed using the Schaefer et al. (2018) 100-ROI cortical parcellation and the Tian (2020) subcortical parcellation. Additional subcortical ROIs were extracted using the Harvard Ascending Arousal Network (periaqueductal gray and parabrachial nucleus), the MNI structural atlas (cerebellum), the California Institute of Technology subcortical atlas (hypothalamus), and the Oxford-Imanova Striatal atlas (ventral striatum). ROIs in the FPN, SN, and DMN were matched to their corresponding subnetworks according to the Yeo et al. (2011) 7-network organization of the cortex. The ROIs in the AIN were selected according to past work which reported the regions composing the AIN (Kleckner et al., 2017) and included 54 ROIs, encompassing the entirety of the DMN and SN, connector hubs in the midcingulate cortex, parahippocampal gyrus, postcentral gyrus, and subcortical structures including the periaqueductal gray, parabrachial nucleus, cerebellum, ventral striatum, and hypothalamus (see Table 1; Fig. 2). The AIN canonically includes the nucleus of the solitary tract as well, but we were unable to include this ROI in our analyses due to poor coverage in our data.

Next, connectivity matrices were obtained by submitting the ROI timeseries to an in-house script written and run in R Statistical Software (v4.2.1; R Core Team, 2022). This script performed linear detrending and normalization on the ROI time series, then computed pairwise Pearson correlations of each ROI timeseries with each other to compute ROIxROI correlation matrices. One correlation matrix was computed for each of the four subnetworks of interest, using only the ROIs contained in that network. This resulted in a 54 × 54 correlation matrix for the AIN, a 24 × 24 correlation matrix for the DMN, a 13 × 13 correlation matrix for the FPN, and a 12 × 12 correlation matrix for the SN. Additionally, a whole-brain correlation matrix was computed for the purpose of calculating participation coefficient measures and exploratory whole-brain measures. In order to compute system segregation between the FPN, SN, and DMN, we created a correlation matrix with the ROIs contained in both the FPN and SN, a correlation matrix with the ROIs contained in both the FPN and DMN, and a correlation matrix with the ROIs contained in both the DMN and SN. All correlation matrices were then z-transformed, any negative correlations were changed to 0 to form a positive matrix, and the positive matrices were proportionally thresholded, such that only the top 10 % of strongest correlations were

Table 1
AIN Nodes.

Node Index	Anatomical Location/Name	Source
1	LH Parietal operculum	Schaefer
2	LH Anterior insula	Schaefer
3	LH Anterior insula	Schaefer
4	LH Dorsolateral prefrontal cortex	Schaefer
5	LH Dorsal anterior cingulate cortex	Schaefer
6	LH Dorsal posterior cingulate cortex	Schaefer
7	LH Premotor cortex	Schaefer
8	LH Middle temporal gyrus	Schaefer
9	LH Middle temporal gyrus	Schaefer
10	LH Angular gyrus	Schaefer
11	LH Angular gyrus	Schaefer
12	LH Pars orbitalis	Schaefer
13	LH Pars orbitalis	Schaefer
14	LH Dorsal anterior cingulate cortex	Schaefer
15	LH Orbitofrontal cortex	Schaefer
16	LH Dorsomedial prefrontal cortex	Schaefer
17	LH Premotor cortex	Schaefer
18	LH Frontal eye field	Schaefer
19	LH Precuneus	Schaefer
20	LH Precuneus	Schaefer
21	RH Secondary visual cortex	Schaefer
22	RH Primary auditory cortex	Schaefer
23	RH Primary motor cortex	Schaefer
24	RH Superior temporal gyrus	Schaefer
25	RH Supramarginal gyrus	Schaefer
26	RH Anterior insula	Schaefer
27	RH Dorsal posterior cingulate cortex	Schaefer
28	RH Premotor cortex	Schaefer
29	RH Temporal pole	Schaefer
30	RH Frontal eye field	Schaefer
31	RH Angular gyrus	Schaefer
32	RH Middle temporal gyrus	Schaefer
33	RH Temporal pole	Schaefer
34	RH Superior temporal gyrus	Schaefer
35	RH Pars orbitalis	Schaefer
36	RH Inferior frontal gyrus	Schaefer
37	RH Ventromedial prefrontal cortex	Schaefer
38	RH Dorsomedial prefrontal cortex	Schaefer
39	RH Frontal eye field	Schaefer
40	RH Precuneus	Schaefer
41	RH Precuneus	Schaefer
42	Periaqueductal gray	Harvard Ascending Arousal Network
43	Parabrachial Nucleus	Harvard Ascending Arousal Network
44	Cerebellum	MNI structural atlas
45	Hypothalamus	California Institute of Technology subcortical atlas
46	Ventral striatum	Oxford-Imanova Striatal
47	RH Hippocampus	Tian
48	RH Amygdala	Tian
49	RH Posterior thalamus	Tian
50	RH Anterior thalamus	Tian
51	LH Hippocampus	Tian
52	LH Amygdala	Tian
53	LH Posterior thalamus	Tian
54	LH Anterior thalamus	Tian

Note: List of nodes included in the AIN and the sources of the ROI masks used in this analysis. PFC=prefrontal cortex; LH=left hemisphere; RH=right hemisphere.

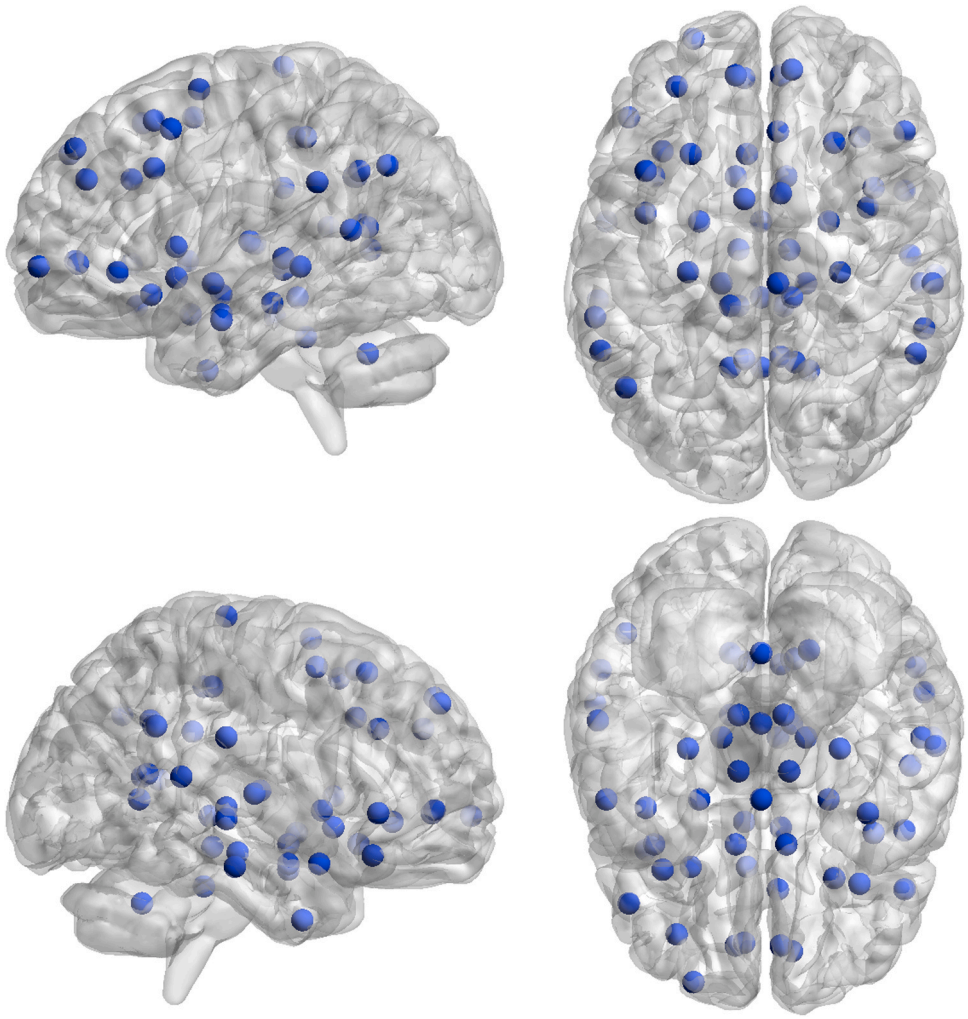

Fig. 2. Visual depiction of nodes of the AIN. Note: AIN=allostatic interoceptive network.

kept. These final connectivity matrices were used to compute graph theory metrics.

Individual graph theory metrics of interest were computed using MATLAB (2022b) scripts from the Brain Connectivity Toolbox (BCT; version 2019–03–03; Rubinov and Sporns, 2010). Global efficiency was computed for each subnetwork as well as the whole-brain network by calculating the average inverse shortest path length between all nodes in the network (or subnetwork). Average participation coefficient was computed within the whole-brain connectivity matrix across all nodes of the AIN and of the FPN by quantifying the diversity of a node's connections to nodes outside of its own network, then averaging across all nodes of each network (AIN or FPN). An additional MATLAB (2022b) script (Chan et al., 2014) was used to compute system segregation between the DMN and FPN, the DMN and SN, and the SN and FPN by calculating the average edge weight of connections between a pair of networks subtracted from the average edge weight of connections within each network as a proportion of the average edge weight of connections within each network.

2.4. Statistical analysis

To account for a positive skew in depressive symptoms, models with depressive symptoms as an outcome were estimated using maximum likelihood estimation with robust standard errors (MLR) through the *lavaan* package (Rosseel, 2012) in R (v4.2.1; R Core Team, 2022). Missing data were handled using full information maximum likelihood (FIML). Seven cases were deleted due to missing data on exogenous variables and one case was deleted due to outliers greater than three standard deviations above the mean on AIN and FPN global efficiency, leaving a final neuroimaging sample size of 109. Sensitivity analyses (see Appendix A) were performed a) with outlier case included and b) controlling for the time between study sessions (T2 and T3). In all cases, results did not differ from those reported in the main manuscript with the exception that inclusion of the outlier case caused the exploratory analysis of mediation by rumination to become marginally significant (see Appendix A).

In the main model, depressive symptoms at T3 were predicted by a set of brain organization metrics collected at T2 including global efficiency of the AIN and FPN, participation coefficient of the AIN and of the FPN, system segregation between the DMN and FPN, and system segregation between the FPN and SN. We controlled for sex, pubertal development score, baseline depressive symptoms at T2, and age at T2. We controlled for age given potential developmental changes in brain organization metrics. We controlled for sex and puberty due to known sex differences in the prevalence and age at onset of depression and links between pubertal development and the development of depression in adolescents (Angold et al., 1998; Joinson et al., 2012). In a follow-up exploratory analysis, trait rumination at T3 was examined as a mediator within the path model. The mediational pathway was tested for significance using bias-corrected non-parametric bootstrapping (1000 iterations) in *lavaan* (Rosseel, 2012).

To assess whether adolescents' adverse peer experiences at T1

prospectively predicted global efficiency of the AIN or segregation between the FPN and SN at T2, we conducted two path analyses. The two path models separately predicted each brain organization metric, with each model including sociometric social preference scores, relational peer victimization, and overt peer victimization as predictors, controlling for age at T1, biological sex, and depressive symptoms at T1. To assess whether adolescents' peer acceptance/rejection or experiences of peer victimization prospectively predicted depressive symptoms, we additionally regressed social preference scores and relational and overt peer victimization on depressive symptoms at T2, while controlling for age at T1, biological sex, and depressive symptoms at T1. In these models, we controlled for age at T1 and biological sex given potential developmental changes in brain organization and both age and sex differences in adverse peer experiences. We also controlled for depressive symptoms at T1 given potential reciprocal and cascading relationships between depression and adverse peer experiences. Three cases were deleted due to missing data on exogenous variables and one case was deleted due to outliers greater than three standard deviations above the mean on AIN and FPN global efficiency, leaving a sample size of 113. As in prior analyses, we found similar effects in sensitivity analyses including the outlier case and controlling for the time between study sessions (see Appendix A).

3. Results

3.1. Brain organization metrics predicting prospective depressive symptoms

See Table 2 for bivariate correlations and descriptive statistics of study variables. Our primary hypotheses focused on brain networks associated with the prospective development of depressive symptoms were preregistered (DOI 10.17605/OSF.IO/VSE4H) and contained age at T2, pubertal development status, sex, depressive symptoms at T2, and all brain organization metrics as predictors of depressive symptoms in T3. Among control variables, depressive symptoms at T2 and age at T2 were significant predictors of depressive symptoms at T3 (β= 0.45, $p < .001$; β= 0.19, $p = 0.014$; see Table 3). Among brain organization metrics, global efficiency of the AIN (β= 0.24, $p = 0.027$) and system segregation between the FPN and SN (β= 0.22, $p = 0.029$) each significantly predicted prospective depressive symptoms at T3 (Table 3). Neither brain organization metric was significantly correlated with head motion during the scan, as defined by mean framewise displacement. In exploratory analyses, we also determined that depressive symptoms at T3 were not predicted by global efficiency of the DMN or SN, segregation between the DMN and SN, or whole-brain global efficiency. Additionally, no brain metrics predicted concurrent depressive symptoms (T2) (see Table 5).

We note that while AIN global efficiency and FPN-SN segregation significantly predicted depressive symptoms in our pre-registered model above, neither had a significant bivariate correlation with depressive symptoms. Upon further examination, we found that AIN global efficiency and FPN-SN segregation act as suppressors for each other's effects, and FPN global efficiency acts as a suppressor for both effects. At a bivariate level, FPN-SN segregation is significantly negatively correlated with AIN global efficiency (r = -0.31, $p < .001$), and AIN global efficiency is significantly positively correlated with FPN global efficiency ($r = 0.35$, $p < .001$). These suppression effects were not explained by the presence of curvilinear effects (e.g., of AIN global efficiency on depression) or significant interactions between AIN global efficiency and either FPN global efficiency or FPN-SN segregation (β= −0.47, $p = 0.56$; β= 0.47, $p = 0.36$), or between FPN global efficiency and FPN-SN segregation (β= 0.65, $p = 0.23$). It is notable that in a model containing whole-brain global efficiency, AIN global efficiency, and control variables, AIN global efficiency significantly predicted prospective depressive symptoms (β= 0.37, $p = 0.049$), and whole-brain global efficiency did not (β= −0.25, $p = 0.24$). Thus, these findings suggest

Table 2
Descriptive statistics and bivariate correlations among main study variables.

Variable	*1*	*2*	*3*	*4*	*5*	*6*	*7*	*8*	*9*	*10*	*11*	*12*	*13*	*14*	*15*	*16*	*17*
1. Timepoint 1 Depressive symptoms	–																
2. Timepoint 2 Depressive symptoms	.26**	–															
3. Timepoint 3 Depressive symptoms	.28**	.44***	–														
4. Timepoint 1 age	.032	−.053	.21*	–													
5. Timepoint 2 age	.089	−.079	.21*	.72***	–												
6. Pubertal development	−.045	−.017	.15	.41***	.40***	–											
7. Biological sex (0 = male, 1 = female)	−.26**	.36***	.20*	−.069	−.078	−.34***	–										
8. AIN global efficiency	.084	−.064	.12	.085	.14	.040	.002	–									
9. FPN participation coefficient	−.11	−.004	−.064	−.061	−.17	−.039	−.13	−.055	–								
10. FPN-SN segregation	.10	.12	.12	.093	.11	−.14	.20*	−.31***	−.20*	–							
11. AIN participation coefficient	−.18	−.14	−.080	−.12	−.18	−.10	−.092	−.020	.41***	−.16	–						
12. FPN global efficiency	−.085	−.12	−.021	−.13	−.045	.033	−.067	.35***	.044	.13	−.019	–					
13. DMN-FPN segregation	.11	.028	−.041	.025	.035	−.067	.059	−.11	−.34***	.13	−.30**	−.13	–				
14. Relational victimization	.16	.29**	.14	−.018	.001	−.009	.022	−.20*	−.10	−.013	−.077	.032	−.038	–			
15. Overt victimization	.23*	.035	.020	.23*	.21*	.19*	−.19*	.076	−.043	−.043	−.15	.14	−.076	.31***	–		
16. Social preference	.065	.061	−.044	.096	.096	.023	.21*	.008	−.066	−.068	−.097	−.972	.094	.017	−.093	–	
17. Rumination	.28**	.26**	.66***	.073	.073	.14	.17	.19	−.065	−.055	−.13	.014	−.12	.14	.037	−.005	–
Mean	2.96	2.92	2.99	12.39	12.99	5.83	–	.27	.14	.72	.34	.13	.54	5.60	4.17	.32	9.96
SD	3.43	3.54	4.16	.58	.56	1.64	–	.040	.020	.19	.030	.030	.17	1.98	1.89	1.22	3.87

Note: Pearson's correlations are presented for all variables except biological sex. Point-biserial correlations are presented for correlations between biological sex and other variables. AIN=allostatic interoceptive network; FPN=frontoparietal network; SN=salience network; DMN=default mode network. *p < . 05, **p < .01, ***p < .001.

Table 3
Results of main analysis model predicting prospective depressive symptoms.

Predictor	*B*	*SE*	*β*	*p*
Initial depressive symptoms	0.55	0.14	0.45	< .001***
Initial age	1.43	0.58	0.19	0.014*
Initial pubertal development	0.27	0.24	0.10	0.26
Biological sex (0 = male, 1 = female)	0.60	0.78	0.069	0.44
AIN global efficiency	27.81	12.57	0.24	0.027*
FPN participation coefficient	−1.04	19.32	−0.005	0.96
FPN-SN segregation	4.98	2.27	0.22	0.029*
AIN participation coefficient	11.22	11.40	0.089	0.33
FPN global efficiency	−14.14	14.28	−0.093	0.32
DMN-FPN segregation	−1.70	2.05	−0.068	0.41

Note: AIN=allostatic interoceptive network; FPN=frontoparietal network; SN=salience network; DMN=default mode network. *p < . 05, **p < .01, ***p < .001.

Table 4
Results of simplified model predicting prospective depressive symptoms.

Predictor	*B*	*SE*	*β*	*p*
Initial depressive symptoms	0.52	0.15	0.43	0.001
Initial age	1.24	0.60	0.16	0.038*
Initial pubertal development	0.28	0.24	0.11	0.24
Biological sex (0 = male, 1 = female)	0.65	0.81	0.076	0.42
AIN global efficiency	27.38	12.45	0.23	0.028*
FPN-SN segregation	4.37	2.14	0.19	0.041*
FPN global efficiency	−11.90	13.66	−0.079	0.38

Note: AIN=allostatic interoceptive network; FPN=frontoparietal network; SN=salience network. *p < . 05, **p < .01, ***p < .001.

Table 5
Results of model predicting concurrent depressive symptoms.

Predictor	*B*	*SE*	*β*	*p*
Biological sex (0 = male, 1 = female)	2.87	0.72	0.40	< .001***
Initial pubertal development	0.43	0.22	0.19	0.054
Initial age	−1.04	0.77	−0.16	0.18
AIN global efficiency	3.13	10.73	0.032	0.77
AIN participation coefficient	−14.90	12.37	−0.14	0.23
FPN global efficiency	−15.57	14.33	−0.12	0.28
FPN participation coefficient	19.70	18.91	0.13	0.30
DMN-FPN segregation	1.21	1.70	0.058	0.48
FPN-SN segregation	2.13	1.67	0.11	0.20

Note: AIN=allostatic interoceptive network; FPN=frontoparietal network; SN=salience network; DMN=default mode network. *p < . 05, ***p < .001.

specific organizational features of the networks in our pre-registered model are meaningful in prospective depression and are not merely indicative of whole-brain global efficiency.

3.1.1. Exploratory mediation by rumination

Building off theoretical links between AIN integration, internal focus, and depression, we conducted an exploratory mediation analysis to further characterize potential pathways by which brain organization metrics prospectively predict depressive symptoms. We tested brooding—an aspect of rumination in which people focus specifically on internal thoughts and sensations—as a potential mediator, which was collected at T3. First, all brain organization metrics and controls were entered as predictors of rumination ($N = 109$), and AIN global efficiency ($\beta = 0.23$, $p = 0.032$) and depressive symptoms at T2 ($\beta = 0.27$, $p = 0.012$) were identified as significant predictors of prospective rumination (Table 6). Again, AIN global efficiency did not have a significant bivariate correlation with rumination, indicating suppression effects. Next, we constructed a path model to test for mediation of the effect of AIN global efficiency on prospective depressive symptoms through rumination. This model included direct paths from all control variables, all brain organization metrics, and rumination to depressive

Table 6
Results of exploratory model predicting rumination.

Predictor	*B*	*SE*	*β*	*p*
Initial depressive symptoms	0.29	0.11	0.27	0.012*
Initial age	0.017	0.78	0.002	0.98
Initial pubertal development	0.35	0.27	0.15	0.20
Biological sex (0 = male, 1 = female)	0.60	0.82	0.078	0.46
AIN global efficiency	24.26	11.30	0.23	0.032*
FPN participation coefficient	8.86	21.79	0.052	0.68
FPN-SN segregation	0.40	2.47	0.019	0.87
AIN participation coefficient	−13.48	10.92	−0.12	0.22
FPN global efficiency	−12.62	18.13	−0.093	0.49
DMN-FPN segregation	−3.38	2.29	−0.15	0.14

Note: AIN=allostatic interoceptive network; FPN=frontoparietal network; SN=salience network; DMN=default mode network. *p < . 05, **p < .01, ***p < .001.

symptoms at T3, as well as an indirect path through rumination for AIN global efficiency and for T2 depressive symptoms (Fig. 3a). This model fit very well across robust fit statistics ($X^2(8) = 6.07$, $p = 0.64$; $CFI = 1.00$; $TLI = 1.06$; $RMSEA = 0.00$, $SRMR = 0.029$) and no modifications were made. In this model, the direct path from AIN global efficiency to depressive symptoms at follow-up was no longer significant, while AIN global efficiency at T2 was a significant predictor of rumination at T3 ($\beta = 0.22$, $p = 0.016$), and rumination at T3 was in turn a significant predictor of depressive symptoms at T3 ($\beta = 0.57$, $p < .001$) (Fig. 3b). This mediational pathway was tested for significance using bias-corrected bootstrapping (1000 iterations), and the indirect effect of AIN global efficiency through rumination was found to be significant ($B = 14.89$, $SE = 7.15$, $p = 0.037$).

3.2. Effects of peer social adversity on brain organization and depressive symptoms

Finally, we examined if experiences of social adversity in peer relationships at T1 prospectively predicted AIN global efficiency or FPN-SN segregation at T2, which occurred an average of seven months later. In our initial model, relational peer victimization significantly prospectively predicted AIN global efficiency ($\beta = 0.21$, $p = 0.033$), such that experiencing more relational peer victimization at T1 was associated with higher global efficiency of the AIN at T2. Neither overt victimization nor social preference score significantly predicted AIN global efficiency (Table 7). In our second model, social preference marginally significantly predicted prospective FPN-SN segregation ($\beta = -0.16$, $p = 0.098$), whereby adolescents who were more socially rejected at T1 had greater segregation between the FPN and SN at T2. Neither relational nor overt victimization significantly predicted FPN-SN segregation (Table 8).

Finally, we tested an exploratory path model examining longitudinal relationships between relational victimization (T1), AIN global efficiency (T2), and depressive symptoms (T3). See Fig. 4 for the full path model ($N = 107$), which had adequate fit across robust fit statistics ($X^2(37) = 52.48$, $p = 0.047$; $CFI = 0.87$; $TLI = 0.81$; $RMSEA = 0.059$, $SRMR = 0.063$). Relational victimization at T1 significantly predicted AIN global efficiency at T2 ($\beta = 0.16$, $p = 0.051$), and AIN global efficiency at T2 subsequently predicted depressive symptoms at T3 ($\beta = 0.23$, $p = 0.037$). However, the indirect path from relational victimization at T1 to depressive symptoms at T3 through AIN global efficiency at T2 was tested for significance using bias-corrected bootstrapping (1000 iterations) was not significant ($B = 0.12$, $SE = 0.099$, $p = 0.22$).

4. Discussion

Adolescence is a period when the onset of depression spikes (Angold et al., 1998; Beesdo et al., 2009; Fergusson et al., 2007; Fleming et al., 1989; Kessler et al., 2005; Lewinsohn et al., 1993; McGee et al., 1992;

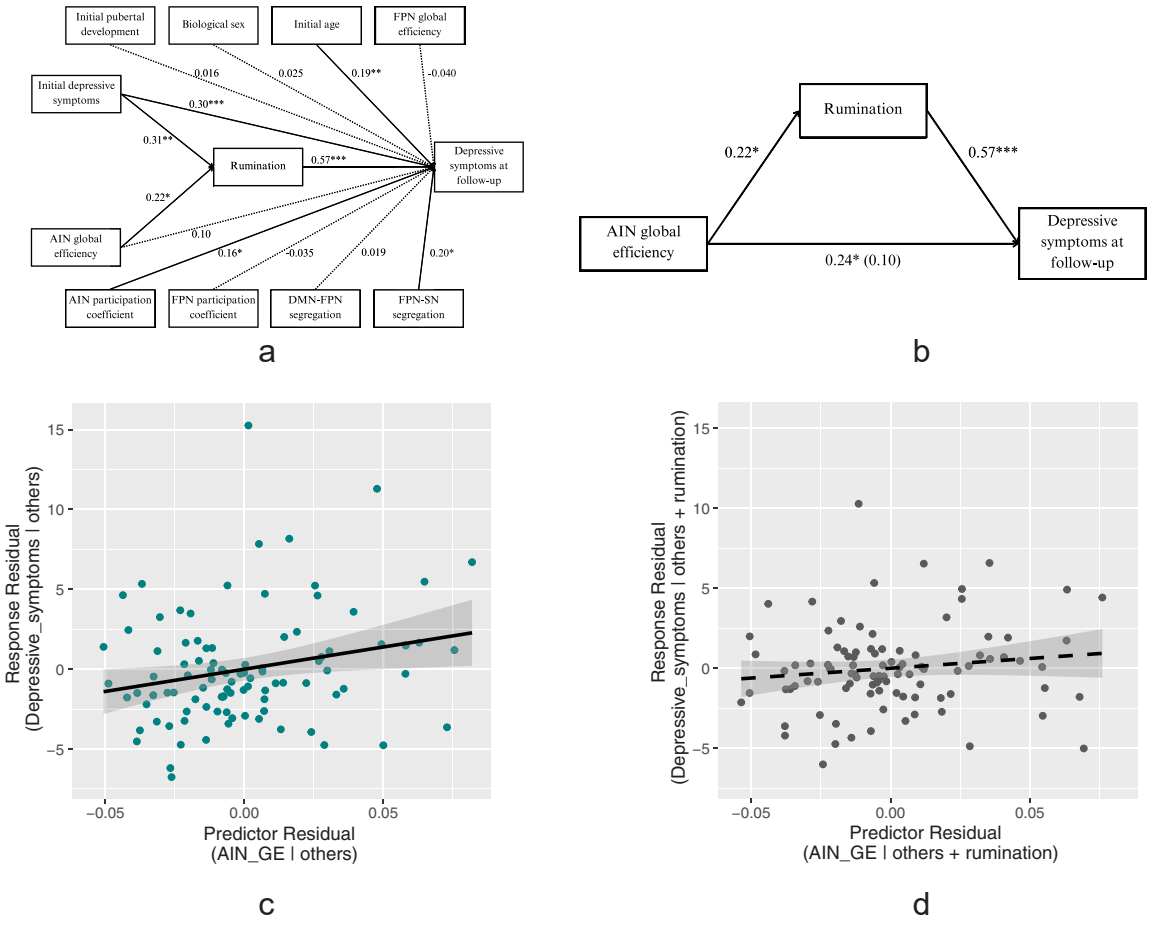

Fig. 3. Path model containing mediation by rumination, mediation by rumination visualized separately and with partial regression plots. Note: AIN=allostatic interoceptive network; FPN=frontoparietal network; SN=salience network; DMN=default mode network; GE=global efficiency. Standardized coefficients are presented. Nonsignificant paths in path diagrams are represented as dotted lines; nonsignificant regression line represented as dashed line. *p < . 05, **p < .01, ***p < .001. A: Path diagram for model containing main model paths as well as mediation by rumination. B: Simplified visualization of mediation pathway from the full model. The standardized estimate of the direct path from AIN global efficiency to depressive symptoms at follow up, controlling for rumination, is in parentheses. C: Partial regression plot showing the unique relationship of AIN global efficiency with depressive symptoms, controlling for all other variables, without rumination included (i.e., visualization of the unmediated relationship or the *c* path). D: Partial regression plot showing the unique relationship of AIN global efficiency with depressive symptoms once rumination is added (i.e., visualization of the *c'* path in the mediation).

Table 7
Results of main model predicting AIN global efficiency.

Predictor	*B*	*SE*	*β*	*p*
Biological sex (0 = male, 1 = female)	< .001	0.007	−0.001	0.99
Initial age	0.006	0.006	0.090	0.35
Timepoint 1 depressive symptoms	< .001	0.001	0.052	0.60
Relational victimization	0.004	0.002	0.21	0.033*
Overt victimization	< .001	0.002	−0.017	0.87
Social preference	< .001	0.003	0.005	0.96

Note: AIN=allostatic interoceptive network. *p < . 05, **p < .01, ***p < .001.

Table 8
Results of main model predicting FPN-SN segregation.

Predictor	*B*	*SE*	*β*	*p*
Biological sex (0 = male, 1 = female)	0.069	0.037	0.18	0.066
Initial age	0.041	0.031	0.12	0.19
Timepoint 1 depressive symptoms	0.004	0.005	0.075	0.45
Relational victimization	−0.003	0.009	−0.034	0.72
Overt victimization	−0.004	0.010	−0.043	0.68
Social preference	−0.024	0.015	−0.16	0.098

Note: FPN=frontoparietal network; SN=salience network; DMN=default mode network. *p < . 05, **p < .01, ***p < .001.

Steinhausen and Winkler Metzke, 2003; Thapar et al., 2012; Joinson et al., 2012) and identifying the social, psychological, and neural factors that prospectively predict depression during this time may help to identify risk factors and move towards a better understanding of the onset of depression in adolescence. Using multi-method longitudinal data collected from adolescents in 6th-8th grade, this study first examined how properties of the functional organization of the AIN—a newly identified large-scale network associated with the etiology of depression (Shaffer et al., 2022)—and the networks associated with the triple network model of psychopathology (including DMN, SN, and FPN) (Menon, 2011) predicted depressive symptoms two years later. We found that global efficiency of the AIN predicted prospective depressive symptoms, such that higher integration within the AIN was associated with greater depressive symptoms at follow-up. We also found that segregation between the FPN and SN predicted prospective depressive symptoms, such that greater segregation between these two networks predicted greater depressive symptoms at follow-up. These brain metrics did not predict concurrent depressive symptoms, suggesting that they represent neural risk factors or indications of a predisposition for developing depressive symptoms.

Our primary models revealed suppression effects whereby AIN global efficiency predicted prospective depression when individual differences in FPN global efficiency and FPN-SN segregation were

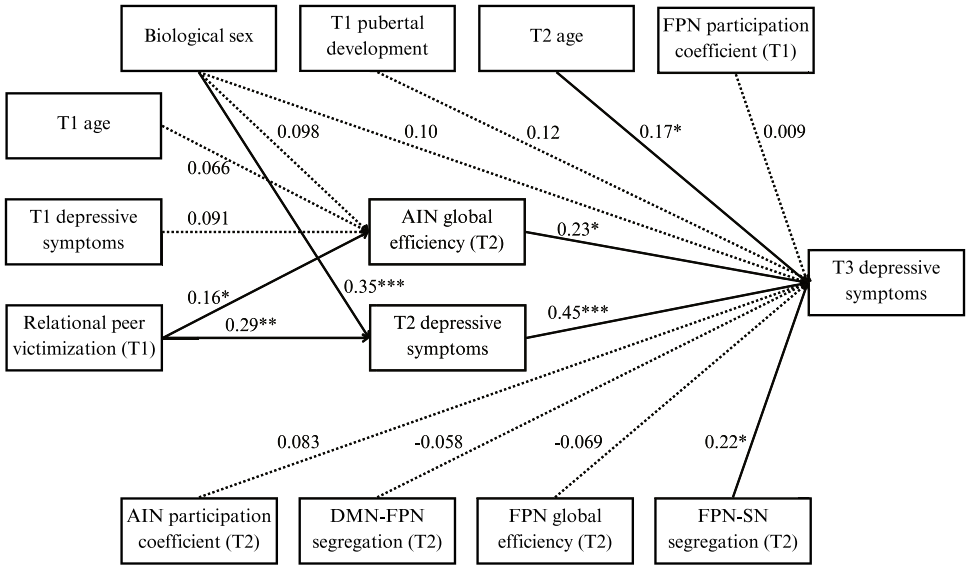

Fig. 4. Path diagram for full path model containing relational victimization, AIN global efficiency, and depressive symptoms. Note: AIN=allostatic interoceptive network; FPN=frontoparietal network; SN=salience network. Nonsignificant paths are represented as dotted lines. *p <. 05, **p < .01, ***p < .001.

accounted for. These suppression effects were not explained by quadratic effects of AIN global efficiency on depression or significant interactions between AIN and FPN global efficiency or FPN-SN segregation. It is possible that subthreshold interactions characterize these effects but require greater statistical power to reveal. We also found that AIN global efficiency predicted depressive symptoms over and above whole-brain global efficiency. Thus, it appears that there is a unique contribution of the AIN in predicting depression that may also depend in some way on how the rest of the brain is functionally organized.

Collectively, these findings are consistent with hypotheses that depression is in part a disorder of dysregulated allostasis (Barrett and Simmons, 2015; Barrett et al., 2016; Shaffer et al., 2022). It is thought that the AIN achieves predictive regulation of the body's metabolic demands by maintaining an internal "model" of the body in the world in order to predictively regulate the body's visceral and motor actions (Barrett et al., 2016; Kleckner et al., 2017). It is possible that greater AIN integration at baseline when considering other aspects of brain organization such as FPN global efficiency may reflect allostatic dysregulation which, over time, manifests as symptoms of depression (dysphoria, anhedonia, fatigue, somatic symptoms).

Our exploratory mediation models suggested that AIN global efficiency may be associated with later depression via an increase in brooding, or repetitive focus on negative thoughts and feelings. This finding is consistent with the idea that greater integration within the AIN may predispose the brain's allostatic model to become overly focused on internal states, which could manifest in rumination as a pattern of maladaptive self-focused thinking.

Our finding that greater segregation between the FPN and SN predicts prospective depressive symptoms is consistent with prior work associating lower connectivity between key nodes in these networks with depression in both adolescents (Connolly et al., 2017; Pannekoek et al., 2014) and adults (Tang et al., 2013; Veer et al., 2010). These findings can also be understood in the context of dysregulated allostasis. The FPN is believed to play a role in allostasis by computing precision weighting of prediction signals generated by the AIN (Shaffer et al., 2022). Thus, Schaffer et al. argue that lower connectivity between nodes in the FPN and SN may also signal weakened precision weighting of predictions that occurs when internal sense data is being overweighted at the expense of sense data from the external world (Shaffer et al., 2022). Thus, our findings may indicate that allostatic dysregulation is contributing to the development of depressive symptoms both through dysregulation of the AIN itself and through weakened precision weighting by the FPN.

4.1. Peer social adversity as a precursor of allostatic dysregulation and depression

In exploratory analyses, we found that adolescents who self-reported having experienced more relational peer victimization had greater AIN integration seven months later. FPN-SN segregation was marginally significantly predicted by sociometrically rated acceptance/rejection from peers, where adolescents who were more socially rejected by their peers had greater segregation between the FPN and SN seven months later.

While we are not able to test the specific mechanisms of the relationship between experiencing relational victimization and greater integration of the AIN, one interpretation is that experiencing relational victimization is a form of stress that can ultimately cause allostatic dysregulation. Consistent with this hypothesis, primates that are excluded from their group mount a host of threat-related responses that are metabolically costly, including inflammatory responses (Cacioppo, Cacioppo, Cole, et al., 2015; see Cacioppo et al., 2014; Cacioppo, Cacioppo, Capitanio, and Cole, 2015 Hawkley and Capitanio, 2015; Hawkley et al., 2012 for reviews). Indeed, adolescents who have experienced peer victimization, particularly relational peer victimization, have been found to have higher c-reactive protein, a biomarker of inflammation (Arana et al., 2018; see Schacter, 2021 for a review). It is also possible that allostatic dysregulation may arise from continual predictions of threat, even after it is no longer acutely present. Together, these findings are consistent with models of social adversity and psychopathology that suggest that adolescents who experience social adversity and then continue to focus or ruminate on that experience are more likely to develop depressive symptoms (Gini et al., 2019; Malamut and Salmivalli, 2023; Mathieson et al., 2014; Peets et al., 2021).

4.2. Conclusion

The results of the present study provide initial evidence for a role of AIN organization in the development of depression and add to existing literature documenting a role of FPN and SN in depression. The highly sensitive developmental timeframe of adolescence examined here, and the longitudinal nature of the data, allows us to capture brain organization patterns that may set the stage for the later development of depressive symptoms. We also found some evidence for factors in the

social environment that predict such patterns, although brain organization did not fully mediate the relationship between social adversity and later depression. Nonetheless, these findings can contribute to our understanding of the social and neural variables that may lead to vulnerability to depression in adolescence before symptoms manifest. Future research should employ a cross-lagged longitudinal design with brain organization, adverse peer experiences, and depressive symptoms at multiple timepoints to examine the full longitudinal causality of social and neural predictors across development. It will also be important to examine the relationship of the AIN and depressive symptoms with other forms of social adversity, such as adversity in the home environment, socioeconomic disadvantage, and experiences of discrimination.

Disclosures

The authors report no conflicts of interest.

Funding

This research was supported by the National Institutes of Mental Health (R01DA039923 to EHT) and the National Science Foundation (BCS 1539651 to EHT).

CRediT authorship contribution statement

Kristen A. Lindquist: Writing – review & editing, Supervision, Project administration, Methodology, Conceptualization. **Tehila Nugiel:** Writing – review & editing, Software, Methodology, Formal analysis. **Frye Natalie Grace:** Writing – review & editing, Writing – original draft, Visualization, Methodology, Formal analysis, Conceptualization. **Mitch J. Prinstein:** Writing – review & editing, Supervision, Project administration, Methodology, Conceptualization. **Gabriella M. Alvarez:** Writing – review & editing, Methodology, Formal analysis. **Eva H. Telzer:** Writing – review & editing, Supervision, Project administration, Methodology, Funding acquisition, Conceptualization. **Jessica R. Cohen:** Writing – review & editing, Methodology, Formal analysis.

Declaration of Competing Interest

The authors declare that they have no known competing financial interests or personal relationships that could have appeared to influence the work reported in this paper.

An author is an Editorial Board Member/Editor-in-Chief/Associate Editor/Guest Editor for this journal and was not involved in the editorial review or the decision to publish this article.

Appendix A. Supporting information

Supplementary data associated with this article can be found in the online version at doi:10.1016/j.dcn.2025.101621.

Data availability

Data will be made available on request.

References

Anderson, M.L. (2010). Neural reuse: A fundamental organizational principle of the brain. Behavioral and Brain Sciences, 33(4), 245–266.https://doi.org/10.1017/S0140525X10000853.

Andrews-Hanna, J.R., Reidler, J.S., Huang, C., Buckner, R.L., 2010. Evidence for the default Network's role in spontaneous cognition. J. Neurophysiol. 104 (1), 322–335. https://doi.org/10.1152/jn.00830.2009.

Angold, A., Costello, E.J., Worthman, C.M., 1998. Puberty and depression: the roles of age, pubertal status and pubertal timing. Psychol. Med. 28 (1), 51–61. https://doi.org/10.1017/S003329179700593X.

Arana, A.A., Boyd, E.Q., Guarneri-White, M., Iyer-Eimerbrink, P., Dougall, A.L., Jensen-Campbell, L., 2018. The impact of social and physical peer victimization on systemic inflammation in adolescents. MerrillPalmer Q. 64 (1), 12–40. https://doi.org/10.13110/merrpalmquar1982.64.1.0012.

Arseneault, L., Bowes, L., Shakoor, S., 2010. Bullying victimization in youths and mental health problems: 'Much ado about nothing'? Psychol. Med. 40 (5), 717–729. https://doi.org/10.1017/S0033291709991383.

Atzil, S., Gao, W., Fradkin, I., Barrett, L.F., 2018. Growing a social brain. Nat. Hum. Behav. 2 (9), 624–636. https://doi.org/10.1038/s41562-018-0384-6.

Barrett, L.F., Satpute, A.B., 2013. Large-scale brain networks in affective and social neuroscience: towards an integrative functional architecture of the brain. Curr. Opin. Neurobiol. 23 (3), 361–372. https://doi.org/10.1016/j.conb.2012.12.012.

Barrett, L.F., Simmons, W.K., 2015. Interoceptive predictions in the brain. Nat. Rev. Neurosci. 16 (7), 419–429. https://doi.org/10.1038/nrn3950.

Barrett, L.F., Quigley, K.S., Hamilton, P., 2016. An active inference theory of allostasis and interoception in depression. Philos. Trans. R. Soc. B Biol. Sci. 371 (1708), 20160011. https://doi.org/10.1098/rstb.2016.0011.

Beckes, L., Coan, J.A., 2011. Social baseline theory: the role of social proximity in emotion and economy of action. Soc. Personal. Psychol. Compass 5 (12), 976–988. https://doi.org/10.1111/j.1751-9004.2011.00400.x.

Beesdo, K., Höfler, M., Leibenluft, E., Lieb, R., Bauer, M., Pfennig, A., 2009. Mood episodes and mood disorders: patterns of incidence and conversion in the first three decades of life. Bipolar Disord. 11 (6), 637–649. https://doi.org/10.1111/j.1399-5618.2009.00738.x.

Cacioppo, J.T., Cacioppo, S., Capitanio, J.P., Cole, S.W., 2015. The neuroendocrinology of social isolation. Annu. Rev. Psychol. 66 (66, 2015), 733–767. https://doi.org/10.1146/annurev-psych-010814-015240.

Cacioppo, J.T., Cacioppo, S., Cole, S.W., Capitanio, J.P., Goossens, L., Boomsma, D.I., 2015. Loneliness across phylogeny and a call for comparative studies and animal models. Perspect. Psychol. Sci. 10 (2), 202–212. https://doi.org/10.1177/1745691614564876.

Cacioppo, S., Capitanio, J.P., Cacioppo, J.T., 2014. Toward a neurology of loneliness. Psychol. Bull. 140 (6), 1464–1504. https://doi.org/10.1037/a0037618.

Chan, M.Y., Park, D.C., Savalia, N.K., Petersen, S.E., Wig, G.S., 2014. Decreased segregation of brain systems across the healthy adult lifespan. Proc. Natl. Acad. Sci. 111 (46), E4997–E5006. https://doi.org/10.1073/pnas.1415122111.

Choukas-Bradley, S., Prinstein, M.J., 2014. Peer relationships and the development of psychopathology. In: Lewis, In.M., Rudolph, K.D. (Eds.), Handbook of Developmental Psychopathology. Springer US, pp. 185–204. https://doi.org/10.1007/978-1-4614-9608-3_10.

Clark, A., 2013. Whatever next? Predictive brains, situated agents, and the future of cognitive science. Behav. Brain Sci. 36 (3), 181–204. https://doi.org/10.1017/S0140525X12000477.

Connolly, C.G., Ho, T.C., Blom, E.H., LeWinn, K.Z., Sacchet, M.D., Tymofiyeva, O., Simmons, A.N., Yang, T.T., 2017. Resting-state functional connectivity of the amygdala and longitudinal changes in depression severity in adolescent depression. J. Affect. Disord. 207, 86–94. https://doi.org/10.1016/j.jad.2016.09.026.

Cowen, E.L., Pederson, A., Babigian, H., Isso, L.D., Trost, M.A., 1973. Long-term follow-up of early detected vulnerable children. J. Consult. Clin. Psychol. 41 (3), 438–446. https://doi.org/10.1037/h0035373.

Crick, N.R., Grotpeter, J.K., 1996. Children's treatment by peers: victims of relational and overt aggression. Dev. Psychopathol. 8 (2), 367–380. https://doi.org/10.1017/S0954579400007148.

Daly, M., 2022. Prevalence of depression among adolescents in the U.S. From 2009 to 2019: analysis of trends by sex, Race/Ethnicity, and income. J. Adolesc. Health 70 (3), 496–499. https://doi.org/10.1016/j.jadohealth.2021.08.026.

Davis, M.M., Navarro, E., Carpenter, K.L.H., Copeland, W.E., Small, B., Egger, H.L., Sheridan, M.A., 2024. Early life adversity and psychopathology in preschoolers: mechanisms and moderators. Eur. Child Adolesc. Psychiatry 33 (6), 1945–1954. https://doi.org/10.1007/s00787-023-02295-5.

Do, K.T., McCormick, E.M., Prinstein, M.J., Lindquist, K.A., Telzer, E.H., 2022. Intrinsic connectivity within the affective salience network moderates adolescent susceptibility to negative and positive peer norms. Sci. Rep. 12 (1), 17463. https://doi.org/10.1038/s41598-022-17780-1.

Esteban, O., Markiewicz, C.J., Blair, R.W., Moodie, C.A., Isik, A.I., Erramuzpe, A., Kent, J. D., Goncalves, M., DuPre, E., Snyder, M., Oya, H., Ghosh, S.S., Wright, J., Durnez, J., Poldrack, R.A., Gorgolewski, K.J., 2019. fMRIPrep: a robust preprocessing pipeline for functional MRI. Nat. Methods 16 (1), 111–116. https://doi.org/10.1038/s41592-018-0235-4.

Fergusson, D.M., Boden, J.M., Horwood, L.J., 2007. Recurrence of major depression in adolescence and early adulthood, and later mental health, educational and economic outcomes. Br. J. Psychiatry 191 (4), 335–342. https://doi.org/10.1192/bjp.bp.107.036079.

Fleming, J.E., Offord, D.R., Boyle, M.H., 1989. Prevalence of childhood and adolescent depression in the community: ontario child health study. Br. J. Psychiatry 155 (5), 647–654. https://doi.org/10.1192/bjp.155.5.647.

Friston, K., 2010. The free-energy principle: a unified brain theory? Nat. Rev. Neurosci. 11 (2), 127–138. https://doi.org/10.1038/nrn2787.

Gini, G., Marino, C., Spada, M.M., 2019. The role of metacognitions and thinking styles in the negative outcomes of adolescents' peer victimization. Violence Vict. 34 (5). Article 5. ⟨https://connect.springerpub.com/content/sgrvv/34/5/752⟩.

Hawkley, L.C., Capitanio, J.P., 2015. Perceived social isolation, evolutionary fitness and health outcomes: a lifespan approach. Philos. Trans. R. Soc. B Biol. Sci. 370 (1669), 20140114. https://doi.org/10.1098/rstb.2014.0114.

Hawkley, L.C., Cole, S.W., Capitanio, J.P., Norman, G.J., Cacioppo, J.T., 2012. Effects of social isolation on glucocorticoid regulation in social mammals. Horm. Behav. 62 (3), 314–323. https://doi.org/10.1016/j.yhbeh.2012.05.011.

Heilbron, N., Prinstein, M.J., 2010. Adolescent peer victimization, peer status, suicidal ideation, and nonsuicidal Self-Injury. MerrillPalmer Q. (Wayne State Univ. Press 56 (3), 388–419. https://doi.org/10.1353/mpq.0.0049.
Henry, T., Asciutto, W., Callenberg, K., kaduffy, 2022. cohenlabUNC/clpipe: clpipe. v1.4.3 (v1.4.3). Zenodo. https://doi.org/10.5281/zenodo.6412959.
Hymel, S., Rubin, K.H., Rowden, L., LeMare, L., 1990. Children's peer relationships: longitudinal prediction of internalizing and externaliziing problems from middle to late childhood. Child Dev. 61 (6), 2004–2021. https://doi.org/10.1111/j.1467-8624.1990.tb03582.x.
Joinson, C., Heron, J., Araya, R., Paus, T., Croudace, T., Rubin, C., Marcus, M., Lewis, G., 2012. Association between pubertal development and depressive symptoms in girls from a UK cohort. Psychol. Med. 42 (12), 2579–2589. https://doi.org/10.1017/S003329171200061X.
Kaiser, R.H., Andrews-Hanna, J.R., Wager, T.D., Pizzagalli, D.A., 2015. Large-Scale network dysfunction in major depressive disorder: a Meta-analysis of Resting-State functional connectivity. JAMA Psychiatry 72 (6), 603–611. https://doi.org/10.1001/jamapsychiatry.2015.0071.
Katsumi, Y., Theriault, J.E., Quigley, K.S., Barrett, L.F., 2022. Allostasis as a core feature of hierarchical gradients in the human brain. Netw. Neurosci. 6 (4), 1010–1031. https://doi.org/10.1162/netn_a_00240.
Kessler, R.C., Berglund, P., Demler, O., Jin, R., Merikangas, K.R., Walters, E.E., 2005. Lifetime prevalence and Age-of-Onset distributions of DSM-IV disorders in The National comorbidity survey replication. Arch. Gen. Psychiatry 62 (6), 593602. https://doi.org/10.1001/archpsyc.62.6.593.
Kind, A.J.H., Buckingham, W.R., 2018. Making Neighborhood-Disadvantage metrics Accessible—The neighborhood Atlas. N. Engl. J. Med. 378 (26), 2456–2458. https://doi.org/10.1056/NEJMp1802313.
Kleckner, I.R., Zhang, J., Touroutoglou, A., Chanes, L., Xia, C., Simmons, W.K., Quigley, K.S., Dickerson, B.C., Feldman Barrett, L., 2017. Evidence for a large-scale brain system supporting allostasis and interoception in humans. Nat. Hum. Behav. 1 (5), 1–14. https://doi.org/10.1038/s41562-017-0069.
Lewinsohn, P.M., Hops, H., Roberts, R.E., Seeley, J.R., Andrews, J.A., 1993. Adolescent psychopathology: I. Prevalence and incidence of depression and other DSM-III—R disorders in high school students. J. Abnorm. Psychol. 102 (1), 133–144. https://doi.org/10.1037/0021-843X.102.1.133.
Lochman, J.E., Wayland, K.K., 1994. Aggression, social acceptance, and race as predictors of negative adolescent outcomes. J. Am. Acad. Child Adolesc. Psychiatry 33 (7), 1026–1035. https://doi.org/10.1097/00004583-199409000-00014.
Malamut, S.T., Salmivalli, C., 2023. Adolescent victimization predicts adult depression and aggression: the role of rumination. Dev. Psychol. 59 (8), 1464–1469. https://doi.org/10.1037/dev0001544.
Mathieson, L.C., Klimes-Dougan, B., Crick, N.R., 2014. Dwelling on it May make it worse: the links between relational victimization, relational aggression, rumination, and depressive symptoms in adolescents. Dev. Psychopathol. 26 (3), 735–747. https://doi.org/10.1017/S0954579414000352.
McGee, R.O.B., Feehan, M., Williams, S., Anderson, J., 1992. DSM-III disorders from age 11 to age 15 years. J. Am. Acad. Child Adolesc. Psychiatry 31 (1), 50–59. https://doi.org/10.1097/00004583-199201000-00009.
McIver, T.A., Bosma, R.L., Sandre, A., Goegan, S., Klassen, J.A., Chiarella, J., Booij, L., Craig, W., 2018. Peer victimization is associated with neural response to social exclusion. MerrillPalmer Q. 64 (1), 135–161.
Menon, V., 2011. Large-scale brain networks and psychopathology: a unifying triple network model. Trends Cogn. Sci. 15 (10), 483–506. https://doi.org/10.1016/j.tics.2011.08.003.
Noble, S., Curtiss, J., Pessoa, L., Scheinost, D., 2024. The tip of the iceberg: a call to embrace anti-localizationism in human neuroscience research. Imaging Neurosci. 2, 1–10. https://doi.org/10.1162/imag_a_00138.
Pannekoek, J.N., van der Werff, S. j a, Meens, P.H.F., van den Bulk, B.G., Jolles, D.D., Veer, I.M., van Lang, N.D.J., Rombouts, S.A.R.B., van der Wee, N.J.A., Vermeiren, R. R.J.M., 2014. Aberrant resting-state functional connectivity in limbic and salience networks in treatment-naïve clinically depressed adolescents. J. Child Psychol. Psychiatry 55 (12), 1317–1327. https://doi.org/10.1111/jcpp.12266.
Peets, K., Turunen, T., Salmivalli, C., 2021. Rumination mediates the longitudinal associations between Elementary-School victimization and Adolescents' internalizing problems. J. Interpers. Violence 37 (17–18), NP16885–NP16906. https://doi.org/10.1177/08862605211025020.
Petersen, A.C., Crockett, L., Richards, M., Boxer, A., 1988. A self-report measure of pubertal status: reliability, validity, and initial norms. J. Youth Adolesc. 17 (2), 117–133. https://doi.org/10.1007/BF01537962.
Prinstein, M.J., 2017. Popular: the power of likability in a Status-obsessed world. Penguin.
Prinstein, M.J., Boergers, J., Vernberg, E.M., 2001. Overt and relational aggression in adolescents: Social-Psychological adjustment of aggressors and victims. J. Clin. Child Adolesc. Psychol. 30 (4), 479–491. https://doi.org/10.1207/S15374424JCCP3004_05.
R. Core Team (2022). R: A language and environment for statistical computing. R Foundation for Statistical Computing, Vienna, Austria. URL ⟨https://www.R-project.org/⟩.
Raichle, M.E., 2015. The Brain's default mode network. Annu. Rev. Neurosci. 38 (38, 2015), 433–447. https://doi.org/10.1146/annurev-neuro-071013-014030.
Reijntjes, A., Kamphuis, J.H., Prinzie, P., Boelen, P.A., van der Schoot, M., Telch, M.J., 2011. Prospective linkages between peer victimization and externalizing problems in children: a meta-analysis. Aggress. Behav. 37 (3), 215–222. https://doi.org/10.1002/ab.20374.
Reijntjes, A., Kamphuis, J.H., Prinzie, P., Telch, M.J., 2010. Peer victimization and internalizing problems in children: a meta-analysis of longitudinal studies. Child Abus. Negl. 34 (4), 244–252. https://doi.org/10.1016/j.chiabu.2009.07.009.
Rosseel, Y., 2012. Lavaan: an r package for structural equation modeling. J. Stat. Softw. 48 (2), 1–36. ⟨http://www.jstatsoft.org/v48/i02/⟩ (URL).
Rubinov, M., Sporns, O., 2010. Complex network measures of brain connectivity: uses and interpretations. NeuroImage 52 (3), 1059–1069. https://doi.org/10.1016/j.neuroimage.2009.10.003.
Rudolph, K.D., Davis, M.M., Monti, J.D., 2017. Cognition–emotion interaction as a predictor of adolescent depressive symptoms. Dev. Psychol. 53 (12), 2377–2383. https://doi.org/10.1037/dev0000397.
Rudolph, K.D., Miernicki, M.E., Troop-Gordon, W., Davis, M.M., Telzer, E.H., 2016. Adding insult to injury: neural sensitivity to social exclusion is associated with internalizing symptoms in chronically peer-victimized girls. Soc. Cogn. Affect. Neurosci. 11 (5), 829–842. https://doi.org/10.1093/scan/nsw021.
Satpute, A.B., Lindquist, K.A., 2019. The default mode Network's role in discrete emotion. Trends Cogn. Sci. 23 (10), 851–864. https://doi.org/10.1016/j.tics.2019.07.003.
Saxbe, D.E., Beckes, L., Stoycos, S.A., Coan, J.A., 2020. Social allostasis and social allostatic load: a new model for research in social dynamics, stress, and health. Perspect. Psychol. Sci. 15 (2), 469–482. https://doi.org/10.1177/1745691619876528.
Schacter, H.L., 2021. Effects of peer victimization on child and adolescent physical health. Pediatrics 147 (1), e2020003434. https://doi.org/10.1542/peds.2020-003434.
Schaefer, A., Kong, R., Gordon, E.M., Laumann, T.O., Zuo, X.-N., Holmes, A.J., Eickhoff, S.B., Yeo, B.T.T., 2018. Local-Global parcellation of the human cerebral cortex from intrinsic functional connectivity MRI. Cereb. Cortex 28 (9), 3095–3114. https://doi.org/10.1093/cercor/bhx179.
Schulkin, J., 2011. Social allostasis: anticipatory regulation of the internal milieu. Front. Evolut. Neurosci. 2. https://doi.org/10.3389/fnevo.2010.00111.
Schulkin, J., Sterling, P., 2019. Allostasis: a Brain-Centered, predictive mode of physiological regulation. Trends Neurosci. 42 (10), 740–752. https://doi.org/10.1016/j.tins.2019.07.010.
Shaffer, C., Westlin, C., Quigley, K.S., Whitfield-Gabrieli, S., Barrett, L.F., 2022. Allostasis, action, and affect in depression: insights from the theory of constructed emotion. Annu. Rev. Clin. Psychol. 18 (18, 2022), 553–580. https://doi.org/10.1146/annurev-clinpsy-081219-115627.
Steinhausen, H.-C., Winkler Metzke, C., 2003. Prevalence of affective disorders in children and adolescents: findings from the zurich epidemiological studies. Acta Psychiatr. Scand. 108 (s418), 20–23. https://doi.org/10.1034/j.1600-0447.108.s418.5.x.
Sterling, P., 2012. Allostasis: a model of predictive regulation. Physiol. Behav. 106 (1), 5–15. https://doi.org/10.1016/j.physbeh.2011.06.004.
Tang, Y., Kong, L., Wu, F., Womer, F., Jiang, W., Cao, Y., Ren, L., Wang, J., Fan, G., Blumberg, H.P., Xu, K., Wang, F., 2013. Decreased functional connectivity between the amygdala and the left ventral prefrontal cortex in treatment-naive patients with major depressive disorder: a resting-state functional magnetic resonance imaging study. Psychol. Med. 43 (9), 1921–1927. https://doi.org/10.1017/S0033291712002759.
Thapar, A., Collishaw, S., Pine, D.S., Thapar, A.K., 2012. Depression in adolescence. Lancet 379 (9820), 1056–1067. https://doi.org/10.1016/S0140-6736(11)60871-4.
Theriault, J.E., Young, L., Barrett, L.F., 2021. The sense of should: a biologically-based framework for modeling social pressure. Phys. Life Rev. 36, 100–136. https://doi.org/10.1016/j.plrev.2020.01.004.
Tian, Y., Margulies, D.S., Breakspear, M., Zalesky, A., 2020. Topographic organization of the human subcortex unveiled with functional connectivity gradients. Nat. Neurosci. 23 (11), 1421–1432. https://doi.org/10.1038/s41593-020-00711-6.
Treynor, W., Gonzalez, R., Nolen-Hoeksema, S., 2003. Rumination reconsidered: a psychometric analysis. Cogn. Ther. Res. 27 (3), 247–259. https://doi.org/10.1023/A:1023910315561.
Tse, N.Y., Ratheesh, A., Tian, Y.E., Connolly, C.G., Davey, C.G., Ganesan, S., Gotlib, I.H., Harrison, B.J., Han, L.K.M., Ho, T.C., Jamieson, A.J., Kirshenbaum, J.S., Liu, Y., Ma, X., Ojha, A., Qiu, J., Sacchet, M.D., Schmaal, L., Simmons, A.N., Zalesky, A., 2024. A mega-analysis of functional connectivity and network abnormalities in youth depression. Nat. Ment. Health 2 (10), 1169–1182. https://doi.org/10.1038/s44220-024-00309-y.
Veer, I.M., Beckmann, C., Van Tol, M.-J., Ferrarini, L., Milles, J., Veltman, D., Aleman, A., Van Buchem, M.A., Van Der Wee, N.J., Rombouts, S.A., 2010. Whole brain Resting-State analysis reveals decreased functional connectivity in major depression. Front. Syst. Neurosci. 4. https://doi.org/10.3389/fnsys.2010.00041.
Vernberg, E.M., 1990. Psychological adjustment and experiences with peers during early adolescence: reciprocal, incidental, or unidirectional relationships? J. Abnorm. Child Psychol. 18 (2), 187–198. https://doi.org/10.1007/BF00910730.
Wang, J., Iannotti, R.J., Luk, J.W., Nansel, T.R., 2010. Co-occurrence of victimization from five subtypes of bullying: physical, verbal, social exclusion, spreading rumors, and cyber. J. Pediatr. Psychol. 35 (10), 1103–1112. https://doi.org/10.1093/jpepsy/jsq048.
Westlin, C., Theriault, J.E., Katsumi, Y., Nieto-Castanon, A., Kucyi, A., Ruf, S.F., Brown, S.M., Pavel, M., Erdogmus, D., Brooks, D.H., Quigley, K.S., Whitfield-Gabrieli, S., Barrett, L.F., 2023. Improving the study of brain-behavior relationships

by revisiting basic assumptions. Trends Cogn. Sci. 27 (3), 246–257. https://doi.org/10.1016/j.tics.2022.12.015.

Wu, B., Li, X., Zhou, J., Zhang, M., Long, Q., 2020. Altered whole-brain functional networks in Drug-Naïve, First-Episode adolescents with major depression disorder. J. Magn. Reson. Imaging 52 (6), 1790–1798. https://doi.org/10.1002/jmri.27270.

Yeo, B.T., Krienen, F.M., Sepulcre, J., Sabuncu, M.R., Lashkari, D., Hollinshead, M., Roffman, J.L., Smoller, J.W., Zöllei, L., Polimeni, J.R., Fischl, B., Liu, H., Buckner, R. L., 2011. The organization of the human cerebral cortex estimated by intrinsic functional connectivity. J. Neurophysiol. 106 (3), 1125–1165. https://doi.org/10.1152/jn.00338.2011.